JVI Journals.ASM.org

Modification of Asparagine-Linked Glycan Density for the Design of Hepatitis B Virus Virus-Like Particles with Enhanced Immunogenicity

Michiko Hyakumura,[a] Renae Walsh,[b] Morten Thaysen-Andersen,[c] Natalie J. Kingston,[a] Mylinh La,[d] Louis Lu,[d] George Lovrecz,[d] Nicolle H. Packer,[c] Stephen Locarnini,[b] Hans J. Netter[a]

Infection and Immunity Program, Monash Biomedicine Discovery Institute and Department of Microbiology, Monash University, Clayton, VIC, Australia[a]; Victorian Infectious Diseases Reference Laboratory, Melbourne, VIC, Australia[b]; Department of Chemistry and Biomolecular Sciences, Macquarie University, Sydney, NSW, Australia[c]; Commonwealth Scientific and Industrial Research Organisation, Clayton, VIC, Australia[d]

ABSTRACT

The small envelope proteins (HBsAgS) derived from hepatitis B virus (HBV) represent the antigenic components of the HBV vaccine and are platforms for the delivery of foreign antigenic sequences. To investigate structure-immunogenicity relationships for the design of improved immunization vectors, we have generated biochemically modified virus-like particles (VLPs) exhibiting glycoengineered HBsAgS. For the generation of hypoglycosylated VLPs, the wild-type (WT) HBsAgS N146 glycosylation site was converted to N146Q; for constructing hyperglycosylated VLPs, potential glycosylation sites were introduced in the HBsAgS external loop region at positions T116 and G130 in addition to the WT site. The introduced T116N and G130N sites were utilized as glycosylation anchors resulting in the formation of hyperglycosylated VLPs. Mass spectroscopic analyses showed that the hyperglycosylated VLPs carry the same types of glycans as WT VLPs, with minor variations regarding the degree of fucosylation, bisecting *N*-acetylglucosamines, and sialylation. Antigenic fingerprints for the WT and hypo- and hyperglycosylated VLPs using a panel of 19 anti-HBsAgS monoclonal antibodies revealed that 15 antibodies retained their ability to bind to the different VLP glyco-analogues, suggesting that the additional *N*-glycans did not shield extensively for the HBsAgS-specific antigenicity. Immunization studies with the different VLPs showed a strong correlation between *N*-glycan abundance and antibody titers. The T116N VLPs induced earlier and longer-lasting antibody responses than did the hypoglycosylated and WT VLPs. The ability of nonnative VLPs to promote immune responses possibly due to differences in their glycosylation-related interaction with cells of the innate immune system illustrates pathways for the design of immunogens for superior preventive applications.

IMPORTANCE

The use of biochemically modified, nonnative immunogens represents an attractive strategy for the generation of modulated or enhanced immune responses possibly due to differences in their interaction with immune cells. We have generated virus-like particles (VLPs) composed of hepatitis B virus envelope proteins (HBsAgS) with additional *N*-glycosylation sites. Hyperglycosylated VLPs were synthesized and characterized, and the results demonstrated that they carry the same types of glycans as wild-type VLPs. Comparative immunization studies demonstrated that the VLPs with the highest *N*-glycan density induce earlier and longer-lasting antibody immune responses than do wild-type or hypoglycosylated VLPs, possibly allowing reduced numbers of vaccine injections. The ability to modulate the immunogenicity of an immunogen will provide opportunities to develop optimized vaccines and VLP delivery platforms for foreign antigenic sequences, possibly in synergy with the use of suitable adjuvanting compounds.

Virus-like particles (VLPs) are tools of a leading innovative bionanotechnology in vector and vaccine development, and they have a number of advantages over traditional vaccines. VLPs do not contain viral genetic material and represent high-density displays of viral structural proteins that efficiently trigger key parts of the immune system for B cell and/or T cell responses (1–3). VLPs composed of the small envelope proteins (HBsAgS) derived from hepatitis B virus (HBV) are the antigenic components of a successful protective vaccine (4, 5). Nevertheless, even with the availability of a vaccine, hepatitis B still represents an enormous health problem. Approximately 2 billion people worldwide have been infected with HBV and more than 240 million individuals have chronic HBV infections. An estimated 780,000 persons die each year from acute or chronic consequences of hepatitis B (6, 7). A cure is not available at present. Therapeutic vaccinations, including the use of dendritic cells (DCs), are procedures under investigation to establish strategies to control the infection (8, 9). The use of biochemically modified HBsAgS VLPs, which induce enhanced immune responses may represent an alternative way to restore potent responses. The HBsAgS VLPs are processed by DCs and antigens presented via the major histocompatibility complex (MHC) class I and II antigen presentation pathways (10). In addition to HBsAgS VLPs being an immunogen of medical interest

Received 2 May 2015 **Accepted** 20 August 2015

Accepted manuscript posted online 2 September 2015

Citation Hyakumura M, Walsh R, Thaysen-Andersen M, Kingston NJ, La M, Lu L, Lovrecz G, Packer NH, Locarnini S, Netter HJ. 2015. Modification of asparagine-linked glycan density for the design of hepatitis B virus virus-like particles with enhanced immunogenicity. J Virol 89:11312–11322. doi:10.1128/JVI.01123-15.

Editor: J.-H. J. Ou

Address correspondence to Hans J. Netter, hans.netter@monash.edu.

Supplemental material for this article may be found at http://dx.doi.org/10.1128/JVI.01123-15.

to prevent or to overcome HBV infections, the particles have been used as platforms for the delivery of foreign antigenic sequences and facilitated the induction of anti-foreign antigen-specific immune responses (11–18). The most advanced malaria vaccine RTS,S is based on HBsAgS VLPs with a circumsporozoite epitope fused to the subunits. The vaccine was safe and showed the ability to prevent cases of clinical malaria (19, 20).

HBV encodes three related envelope transmembrane proteins (HBs): HBsAg-large (HBsAgL), -middle (HBsAgM) and -small (HBsAgS). The proteins share a region known as the S-domain. HBsAgS is composed only of the S-domain, consisting of 226 amino acids (aa); HBsAgM and -L contain additional N-terminal extensions, the preS2 and preS1 domains. The first step in particle morphogenesis is the cotranslational insertion of HBsAgS into the endoplasmic reticulum (ER) membrane of the host cell with a short luminal exposed N-terminal sequence, two transmembrane regions separated by a 57-aa cytosolic loop, and a luminal external hydrophilic loop (major hydrophilic region) between residues 99 and 169. The external hydrophilic region contains multiple epitopes, including an immunodominant ("a"-determinant) region that is common to all HBV genotypes. Based on a topological model, the external hydrophilic region is represented by a two-loop structure defined by disulfide bridges, with the first loop formed by residues 100 to 138 and the second loop by residues 139 to 146 (21–23). HBsAgS proteins in the absence of any other viral gene product have the ability to assemble into lipid containing VLPs with a diameter of 22 to 25 nm. The particles represent a highly compact structure due to the large number of intra- and intermolecular disulfide bonds within and between the proteins (21–26). The three envelope proteins can be glycosylated at residue N146 (via *N*-glycosylation) in the S-domain, but approximately half the molecules remain unglycosylated due to an underutilization of this site. The presence of a single glycan at position N146 increases the molecular mass of HBsAgS from 24 kDa to approximately 26 to 28 kDa. Three different glycan structures were identified on subviral particles: biantennary, fucosylated biantennary, and triantennary structures (27–29). The synthesis and secretion of HBsAgS VLPs do not depend on *N*-glycosylation, in contrast to the formation and release of infectious HBV particles (30–33).

The use of biochemically modified HBsAgS VLPs represents a design pathway to generate immunogens with modulated or enhanced immunogenicity, possibly allowing the development of tools suitable for therapeutic approaches or superior platforms. In an attempt to enhance the VLP immunogenicity, biochemically modified VLPs were generated with a reduced level of disulfide bonding to weaken the particulate structure and to promote antigen processing (34). The modification of the disulfide bonding pattern possibly influences antigen processing and epitope selection via the MHC class II pathway (35, 36). Similarly, changes in disulfide bonding influenced cross-presentation of a human malaria cytotoxic T lymphocyte (CTL) epitope (37). As an alternative approach, the design of improved vaccines exploits the recognition of glycans by glycan-binding proteins. Glycan-mediated interactions with immunocompetent cells impact protein antigen uptake and enhance cell-mediated and humoral immune responses (38–40), but they also have the ability to promote viral escape by shielding epitopes to evade neutralizing antibodies, and they can sterically block antigen processing (41, 42). The interaction of immunogens with antigen-presenting cells such as DCs is influenced by the glycosylation status of the immunogen, and it has become evident that the glycan presentation and their density influence recognition by lectins (43).

Different classes of glycan-binding proteins are involved in glycoprotein recognition, with profound effects on the activation of the adaptive immune response. Manipulation of protein glycosylation has been recognized as a strategy to promote antigen internalization and antigen presentation via MHC class I and class II molecules promoting cellular and humoral immune responses (44). Targeting the mannose receptor, a C-type lectin, showed that mannosylation provided an efficient strategy to improve antigen uptake, processing, and presentation. Mannosylation enhanced uptake of VLPs by antigen-presenting cells (38), and also enhanced the cell-mediated and humoral immunogenicity of immunogens (40, 45–47). Mannosylated solid lipid nanoparticles loaded with HBsAg induced stronger cellular responses than nanoparticles devoid of mannose (48). Similarly, glycosylated tumor associated antigens induced enhanced immune responses (39).

Protein glycosylation patterns are defining structural elements that contribute to particle uptake and processing by antigen-presenting cells. Using rational design, we have generated hyperglycosylated HBsAgS VLPs to develop immunogens with enhanced or modulated immunogenicity. To investigate whether differentially glycosylated VLPs vary in their antigenicity and immunogenicity, additional *N*-glycosylation consensus sequences (sequons) were introduced to produce hyperglycosylated VLPs, and the anti-HBs immune response was measured. We hypothesize that nonnative differentially glycosylated VLPs interact differently with the immune system than do wild-type (WT) VLPs, and we show that they have the ability to induce an accelerated B cell immune response. The design of nonnative immunogens and the careful selection of novel glycosylation sites may permit the development of innovative approaches to generate superior preventive immunogens.

MATERIALS AND METHODS

***In vitro* SDM.** Expression plasmids (p-HBs-T116N and p-HBs-G130N) based on the pCI vector (Promega, Madison, WI) encoding HBsAgS proteins (genotype D, serotype ayw) with T116N and G130N amino acid substitutions were constructed. The mutations T116N and G130N generated consensus *N*-glycosylation sites 116-N-S-T-118 and 130-N-T-S-132, respectively. Plasmids p-HBs-WT and p-HBs-N146Q encode HBsAgS proteins with and without the WT glycosylation site, respectively. Site-directed mutagenesis (SDM) was performed with pairs of complementary primers introducing the appropriate mutations. The following conditions were applied: *Pfu* DNA polymerase (1 μl, 10 U/μl) in the recommended buffer (Promega), a 100 μM concentration of each deoxynucleoside triphosphate (dNTP), 1 μM primer pair, and 50 ng of a template in a total volume of 50 μl. The extension reaction was initiated by a preheating step at 95°C for 1 min, followed by 18 cycles of 95°C for 30 s, 60°C for 1 min, and 68°C for 15 min and then a final step at 68°C for 7 min. The reaction sample was treated with 1 μl of DpnI (10 U/μl) restriction enzyme (Promega) for 1 h at 37°C and then the DNA products used for transformation of *Escherichia coli* DH5α cells. Colonies were grown in the presence of ampicillin (100 μg/ml) on Luria-Bertani agar plates. Plasmids were isolated and verified by sequencing.

Cell lines. The HEK293T cell line was grown in Dulbecco's modified Eagle's medium (DMEM; Gibco-BRL, Grand Island, NY) supplemented with GlutaMax-1 (Gibco-BRL), 10% fetal calf serum (FCS), and penicillin and streptomycin (Gibco-BRL). For the production of VLPs, HEK293T cells were transfected using polyethylenimine (25 kDa, linear) (PEI; Poly-

sciences, Warrington, PA). The VLPs were harvested from the cell culture supernatant 5 days posttransfection.

Purification and quantitation of VLPs. The collected tissue culture supernatant was centrifuged using a benchtop centrifuge, then the supernatant was transferred into an ultracentrifuge tube, underlaid with a 20% sucrose cushion, and the particles pelleted by ultracentrifugation as described by Cheong et al. (12). The supernatant was discarded, and the pelleted VLPs were resuspended in sodium-Tris-EDTA (STE) buffer (100 mM NaCl, 10 mM Tris [pH 8], 1 mM EDTA) for vaccination purposes. The presence of HBsAgS was assessed using a Monolisa Ultra assay according to the manufacturer's instructions (Bio-Rad, Hercules, CA).

EM analysis. Partially purified VLPs were further purified through a 10 to 40% (wt/vol) sucrose gradient in STE buffer for electron microscopy (EM) analysis. Fractions were collected and measured using an HBsAg-specific enzyme-linked immunosorbent assay (ELISA) (Monolisa; Bio-Rad). The refractive index of each fraction was measured using an Abbe refractometer (NAR-1T; Atago, Tokyo, Japan). Fractions containing HBsAgS were dialyzed against phosphate-buffered saline (PBS). Ten microliters of sample was applied to a carbon grid, blotted, and negatively stained with phosphotungstic acid (PTA). Images were analyzed on a Hitachi H7500 electron microscope (Tokyo, Japan) operating at 120 keV, at Monash Micro Imaging, Monash University, Victoria, Australia.

Immunoprecipitation and gel electrophoresis of HBsAgS proteins. HEK293T cells (5×10^5 cells/ml) were seeded into six-well plates and transfected using the reagent PEI (Polysciences) 2 days prior to the isotopic labeling. The cell culture medium was removed, and then 1.5 ml of methionine-free minimal essential medium was added to the cells. After 40 min, 200 μCi of [^{35}S]methionine-cysteine was added to the medium and incubated for 3 h, washed twice in PBS, and incubated for up to 18 h with 2 ml of DMEM supplemented with 10% FCS. Cell culture medium was harvested and cells were isolated, lysed in lysis buffer (50 mM Tris HCl [pH 7], 250 mM NaCl, 5 mM EDTA, and 1% NP-40), kept on ice for 10 min, and then spun for 10 min at 10,000 × *g* to remove the debris, and the lysate supernatant was taken. Iodoacetamide was added to a final concentration of 20 mM to the collected cell culture and lysate supernatants, followed by incubation with rabbit anti-HBsAg antibodies (Meridian Life Science, Memphis, TN) diluted to 1:500 for 2 h on ice, and 1 h of incubation with 20 μl of protein A Sepharose CL-4B (GE Healthcare, Piscataway, NJ) at 4°C with rotation. The mixture was washed three times in radioimmunoprecipitation assay (RIPA) buffer (10 mM Tris-HCl [pH 7.5]), 150 mM NaCl, 1% [vol/vol] NP-40, 1% ([wt/vol] sodium deoxycholate, 0.1% ([wt/vol] sodium dodecyl sulfate [SDS]) and once with 0.1 M Tris-HCl (pH 6.8). For digestion with peptide-*N*-glycosidase F (PNGase F), aliquots of ^{35}S-labeled HBsAgS VLPs were incubated for 5 min at 95°C in the presence of glycoprotein denaturing buffer containing 0.5% SDS and 40 mM dithiothreitol (DTT) and then digested overnight with PNGase F at 37°C in the presence of 50 mM sodium phosphate (pH 7.5) and 5% NP-40 (New England BioLabs, Ipswich, MA). Samples were prepared for SDS-15% polyacrylamide gel electrophoresis (PAGE) by adding loading buffer (250 mM Tris-HCl [pH 6.8], 8% SDS, 0.4% [wt/vol] bromophenol blue, 40% [vol/vol] glycerol, 20% [vol/vol] 2-mercaptoethanol) and then boiled for 5 min. After electrophoresis, the gel was destained in 7.5% acetic acid–5% methanol and dried before exposure to a BioMax film (Kodak, Rochester, NY) or a Typhoon phosphorimager (GE Healthcare).

Animals and immunization procedure. BALB/c mice were used at 8 to 10 weeks of age. Mice were housed under pathogen-free conditions. Groups of eight female mice were immunized subcutaneously at the base of the tail with 2 μg of WT or biochemically modified HBsAgS VLPs in the absence of an adjuvant. The mice were immunized four times in 2-week intervals (week 1, 3, 5, and 7), and serum samples were taken at weeks 2, 4, 6, and 8 and then from week 9 every week until week 16 (final bleed). The antibody responses were measured by an ELISA using yeast-derived HBsAgS VLPs (serotype ayw; Meridian Life Science) as targets. GraphPad Prism was used for statistical analysis; statistical significance of differences between groups was calculated using two-way analysis of variance (ANOVA) (a P value of <0.05 was considered significantly different).

Multiplex immunoassay. A Bio-Plex bead-based flow cytometric platform (Bio-Rad) was used to develop an HBsAg fingerprinting assay and to establish and map the antigenic profile of the HBsAgS VLPs (49). Briefly, the HBsAgS multiplex immunoassay comprises panels of fluorescently labeled beads, each set conjugated to a different anti-HBV envelope antibody, which binds the HBsAgS VLPs, and a polyclonal phycoerythrin-conjugated detector antibody. The HBsAgS multiplex panel consists of 19 monoclonal antibodies (MAbs) directed against the N terminus, the external hydrophilic loop region, and C-terminal domain epitopes spanning amino acid residues 99 to 226 of HBsAgS. MAbs 1, 2, 3, and 4 (6H6B6, 27E7F10, F4-7B, and 2G2G10, respectively) were kindly provided by Béatrice Seignères, bioMérieux (50, 51), MAbs 18 and 19 were from XTL Biopharmaceuticals (52), MAbs 5, 6, 7, 8, and 9 (RFHBS 1, 2, 4, 7, and 18, respectively) were kind gifts from Howard Thomas, Imperial College London (53), and MAbs 10-17 were kindly provided by Thomas Leary, Abbott Diagnostics (54). The epitopes are categorized into the following domains: N terminal (MAb 1), loop 1 (MAbs 5, 6, and 10), loop 2 (MAbs 7, 8, 11, 12, 16, 17, and 19), loop 1/2 combinational (MAbs 13, 14, and 15), C terminal (MAbs 2, 3, and 4), and conformational (MAbs 9 and 18). The phycoerythrin intensity provides a sensitive measure of antibody recognition of a specific HBsAg epitope within the VLP. The epitope profile of HBsAgS VLPs in comparison to the matched WT backbone was expressed as fold change in antibody binding and epitope recognition using bioinformatics data analysis. VLP data were further normalized to the WT HBsAgS VLP for specific analysis of the effect of HBsAg glycosylation variant VLPs. The 95% consistency index (CI) for the normal range of variation of epitope recognition from the reference backbone was established as ±0.5-fold change. A gain-of-epitope recognition corresponds to positive fold change (>0.5-fold), and negative fold changes (>0.5-fold) correspond to a loss or reduction of epitope binding.

***N*-Glycome profiling of HBsAgs.** *N*-Glycans were released from purified WT and modified HBsAg VLPs using the protocol outlined by Jensen et al. (55). Briefly, equimolar amounts of the HBsAgS variants (~500 pmol) were spotted on polyvinylidene difluoride (PVDF) membranes and stained with Direct blue (Sigma-Aldrich, St. Louis, MO). The membrane spots were excised and washed in separate wells in a flat-bottom polypropylene 96-well plate (Corning Incorporated, NY). *N*-linked glycans were released from the membrane proteins using 3 U of PNGase F (Roche Diagnostics, Basel, Switzerland), with overnight incubation at 37°C. Released *N*-glycans were reduced using 20 μl of 1 M $NaBH_4$ in 50 mM KOH for 3 h at 50°C. Reactions were quenched using 2 μl of glacial acetic acid, desalted using AG 50W-X8 cation-exchange resins (Bio-Rad) packed in empty Top-tips. The *N*-glycans were dried by vacuum centrifugation and washed repeatedly with 100 μl of methanol, with drying by vacuum centrifugation after every wash. The *N*-glycans were desalted further as described previously (55) and finally resuspended in 10 μl of water and subjected to porous graphitized carbon liquid chromatography-electrospray ionization-tandem mass spectrometry (PGC-LC-ESI-MS/MS).

PGC-LC-ESI-MS/MS characterization of *N*-glycans. *N*-Glycans were separated on a Hypercarb PGC column (5-μm particle size, 320 μm [inside diameter] by 10 cm; Thermo Scientific) on an Agilent 1100 capillary LC (Agilent Technologies, Santa Clara, CA) and analyzed using an Agilent MSD three-dimensional ion-trap XCT Plus mass spectrometer coupled directly to the LC. Separation was carried out at a constant flow rate of 2 μl/min using a linear gradient of 2 to 16% (vol/vol) acetonitrile–10 mM NH_4HCO_3 for 45 min, followed by a gradient from 16 to 45% (vol/vol) acetonitrile–10 mM NH_4HCO_3 over 20 min before washing the column with 45% (vol/vol) acetonitrile–10 mM NH_4HCO_3 for 6 min and reequilibrating in 10 mM aqueous NH_4HCO_3. MS/MS was set up with a drying gas temperature of 325°C and a drying gas low of 7 liters/min and nebulizer gas at 18 lb/in^2. Skimmer, trap drive, and capillary exit were set at −40 V, −99.1 V, and −166 V, respectively. Smart fragmentation was used with 30% start and 200% end amplitudes, a maximum accumulation time

of 200 ms, and an ion target of 100,000 ions. ESI-MS was performed in negative-ion mode with two scan events: MS full scan (*m/z* 100 to 2,200) with a scan speed of 8,100 *m/z*/s and data-dependent MS/MS scan after collision-induced dissociation (CID) of the top two most intense precursor ions with a threshold of 30,000 and a relative threshold of 5% relative to the base peak. Dynamic exclusion was inactivated. All precursors were observed in charge state −1 and/or −2. The instrument was calibrated prior to acquisition. The deviations of the observed molecular masses from the theoretical masses were generally below 0.2 Da.

***N*-Glycome data analysis.** Raw MS data were viewed using ESI-compass 1.3 Bruker Daltonic software, and the glycan molecular masses and their individual structures were manually assigned. The list of *N*-glycans was initially filtered to only include species for which clear isotopic patterns with monoisotopic masses matching a known monosaccharide composition (http://www.expasy.ch/tools/glycomod) and/or where interpretable MS/MS spectra were available. From this, the glycan structures could be characterized from (i) accurate molecular mass, (ii) MS/MS partial *de novo* sequencing, and (iii) PGC-LC retention time. MS/MS fragmentation profiles were matched to *in silico* fragments, and the fragmentation pattern was compared qualitatively to MS/MS profiles of identical structures using published data sets (56, 57). GlycoWorkbench was additionally employed (http://www.eurocarbdb.org/applications/ms-tools) to assist in assigning the glycan structure using *in silico* fragmentation analysis. The distribution of *N*-glycans of WT and glycosylation variants of HBsAgS was mapped using the MS signal strength of the observed *N*-glycan structures as an estimate of their relative abundances (58, 59). This was performed using the areas of the extracted ion chromatograms (EIC) of all the charge states in which the identified *N*-glycans appeared. Only *N*-glycans which fulfilled the above-mentioned criteria and were present in more than 0.5% of the total glycome from at least one of the HBsAgS variants were included in the quantitative assessment; the remainder of the structures were not included in the quantitation and were presented as trace. The *N*-glycomes of all HBsAgS variants were analyzed twice by technical replicates. The relative *N*-glycan abundance of WT and glycosylation variants of HBsAgS was assessed by their total (summed) EIC areas of all observed *N*-glycans when equimolar amounts of HBsAgS forms were analyzed.

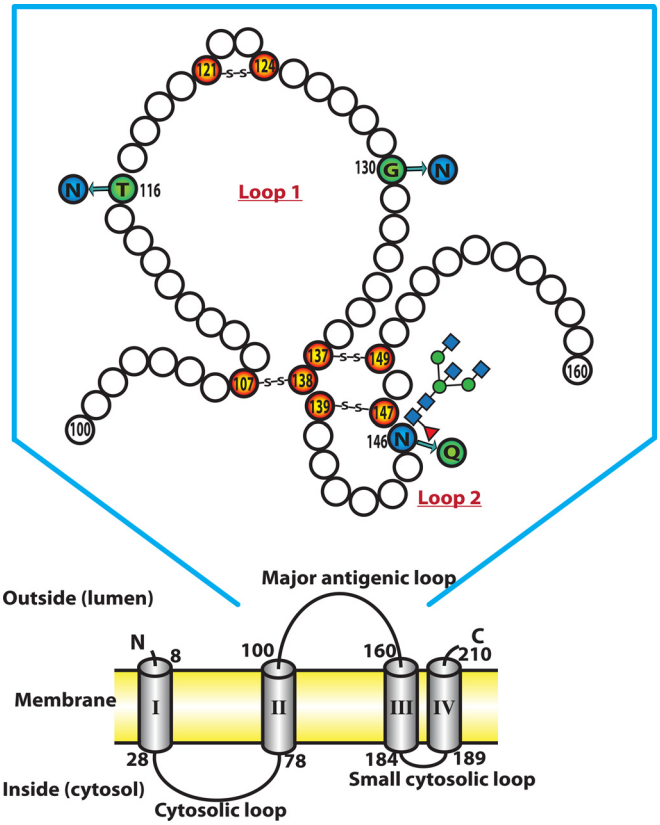

FIG 1 Schematic diagram of HBsAgS. Wild-type (WT) HBsAgS has glycosylation site at amino acid (aa) 146. To introduce new potential glycosylation sites, site-directed mutagenesis was performed at positions T116 and G130 to introduce an asparagine (N) in a NXT/S sequon. Cysteine residues are indicated by orange circles, and disulfide bonds are indicated by "-S-S-." Alpha-helix transmembrane regions are shown as cylinders.

RESULTS

Generation and characterization of differentially glycosylated HBsAgS VLPs. To generate nonnative particulate immunogens, novel *N*-glycosylation sequons were introduced at HBsAgS amino acid (aa) 116 and 130 in addition to the WT glycosylation site at asparagine 146. The HBsAgS amino acid residues threonine and glycine at aa 116 and 130 were replaced with asparagine to generate the T116N and G130N-HBsAgS proteins, respectively (Fig. 1) to introduce novel glycosylation sites at different locations within the external antigenic loop. To generate HBsAgS VLPs in the absence of the WT glycosylation site, the N146 was replaced with a glutamine residue (N146Q-ΔHBsAgS).

The corresponding expression plasmids were transfected into HEK293T cells to produce VLPs in a cell line allowing high-yield protein production, and the cell culture medium was harvested to monitor the presence of secretion competent VLPs. Immunoprecipitation of ^{35}S-labeled VLPs with a polyclonal anti-HBsAgS antibody demonstrated that the T116N- and G130N-HBsAgS proteins produced hyperglycosylated VLPs, as indicated by the increased molecular mass (Fig. 2A and B). The position of the introduced glycosylation site influenced the efficiency of glycosylation, resulting in T116N VLPs composed of subunits which are predominantly mono- or diglycosylated. G130N VLPs are composed of unglycosylated and mono- and diglycosylated HBsAgS subunits. Consistently, the T116N diglycosylated subunits show a slightly higher molecular mass than the G130N diglycosylated subunits, possibly influenced by differences in the glycan composition and/or differences in conformational constraints (Fig. 2A). As expected, the deletion of the glycosylation site 146 (N146Q) resulted in VLPs composed of nonglycosylated 24-kDa subunits. Treatment of the glycosylated HBsAgS VLPs with PNGase F removed the glycan residues resulting in de-*N*-glycosylated HBsAgS subunits of 24 kDa (Fig. 2C and D). Analyzing particle formation and integrity by electron microscopy showed that WT, N146Q-ΔHBsAgS, T116N- and G130N-HBsAgS subunits assemble into particles with a diameter between 22 and 30 nm and with similar morphology (Fig. 3). Density measurements using a CsCl gradient demonstrated that the VLPs, regardless of the glycosylation status, had a density of 1.2 g/ml, consistent with VLPs composed of WT HBsAgS proteins (data not shown) (60, 61). The data demonstrate the formation of biochemically modified VLPs with an increased glycosylation site occupation and higher glycan density.

The selected mutations T116N and G130N occur rarely in HBV variants and also represent only a subset of the virus population. The analysis of 1556 HBsAgS-specific DNA sequences extracted from a HBV database (SeqHepB) (34, 62) revealed that asparagine at position 116 or 130 is present in <1% of the naturally occurring sequences. The amino acids threonine at position 116 and glycine at position 130 are conserved in 99.5% and 98% of

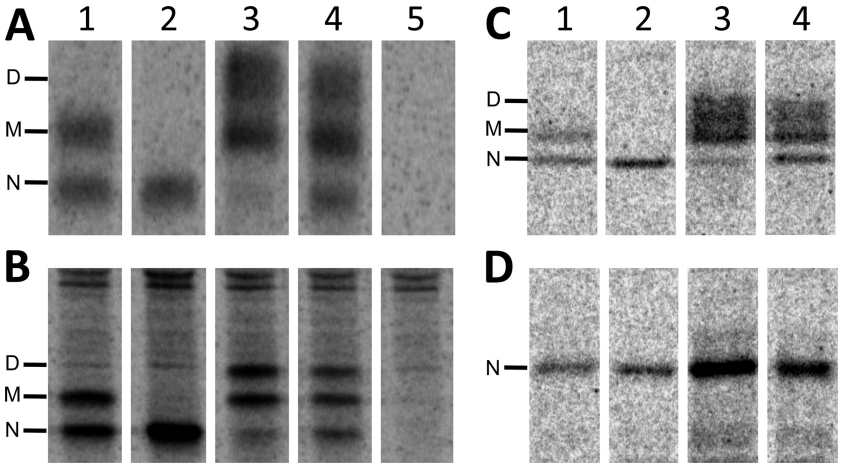

FIG 2 To identify the synthesis of differentially glycosylated virus-like particles (VLPs), HEK293T cells were transfected with plasmids expressing the VLP subunits, HBsAgS. The culture supernatant (A) and the cell lysate (B) were harvested, [^{35}S]methionine-cysteine-labeled VLPs were immunoprecipitated with anti-HBsAgS antibodies, and the HBsAgS subunits were separated by gel electrophoresis under reducing conditions. To verify the presence of *N*-glycans, [^{35}S]methionine-cysteine-labeled VLPs from the cell culture supernatant were immunoprecipiated (C) and digested with PNGase F (D) and then separated by gel electrophoresis and visualized. Lane 1, VLPs composed of wild-type HBsAgS subunits with the N146 glycosylation site present. Lane 2, N146 glycosylation site (N146Q) of HBsAgS removed. Lanes 3 and 4: VLPs composed of HBsAgS subunits with introduced glycosylation sites at positions T116N and G130N, respectively. In addition to the newly introduced sites, the N146 glycosylation site is retained. Lane 5, samples derived from cells transfected with the empty pCI vector. N, M, and D, nonglycosylated (24-kDa), monoglycosylated (27-kDa), and diglycosylated (30/31-kDa) HBsAgS proteins, respectively.

the analyzed sequences, respectively. Based on the *ex vivo* clinical sera data and clinical data, no correlation between the occurrence of the mutations to a disease outcome can be made.

Identification of the *N*-glycans present on the N146Q-ΔHBsAgS, T116N VLPs, G130N VLPs, and WT VLPs. To determine the total abundance of the glycan structures attached to the VLPs, the amount of HBsAgS *N*-glycosylation was determined by combining the liquid chromatography mass spectrometric (LC-MS) intensity of the total observed *N*-glycans normalized to the HBsAgS protein amount used for the *N*-glycome analysis (Fig. 4A). The protein-normalized *N*-glycan abundance calculated from the MS data corresponded to the degree of glycosylation shown by the immunoprecipitation study: the T116N VLPs, composed of mono- and diglycosylated HBsAgS subunits and a small fraction of unglycosylated forms, showed the highest glycan abundance on the protein, followed by the G130N VLPs, which displayed more unglcosylated isoforms, and then WT VLPs, which appear only approximately 50% glycosylated on the native N146 site (Fig. 2 and 4A). The N146Q-ΔHBsAgS VLP variant contained trace but still detectable levels of *N*-glycosylation, primarily of high-mannose type (Fig. 4B, structure 22). WT VLPs as well as the hyperglycosylated VLPs illustrated an extensive microheterogeneity (57 *N*-glycan monosaccharide compositions and 102 unique *N*-glycan structures) with core fucosylation (α1,6), terminating bisecting (β1,4) and antenna (β1,2) *N*-acetylglucosamine (GlcNAc), and sialylation (α2,3 and α2,6) as dominating features (Fig. 4B and C; see also Table S1 in the supplemental material). Analyzing the features of the *N*-glycan structures of WT, T116N, and G130N VLPs showed that the presence of additional *N*-glycosylation sites did not substantially change the nature of the *N*-glycans, as indicated by the relative distribution of the glycan structures. The similarity of glycan types was demonstrated by the high correlation coefficient of the *N*-glycomes of the WT versus T116N (R^2 = 0.827) and the WT versus G130N (R^2 = 0.923) (Fig. 4C; see also Table S1 in the supplemental material). Bisecting-type glycans remain forming the greatest percentage of the structures on all VLPs (Fig. 4B). Slight differences in the fine structure of the glycans were observed, showing that T116N and G130N VLPs have more core fucosylation and less Lewis-type fucosylation, sialylation, and bisecting GlcNAc (data not shown). The observation that T116N- and G130N-HBsAgS VLPs have a higher level of total glycosylation in comparison to the WT HBsAgS VLPs demon-

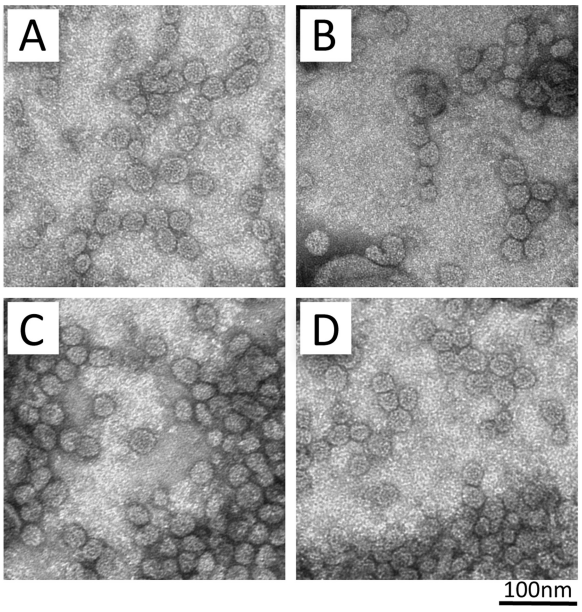

FIG 3 Electron micrograph of VLP samples. VLPs were derived from the cell culture medium and purified by sucrose density gradient centrifugation, dialyzed against phosphate-buffered saline (PBS), and visualized by negative staining with phosphotungstic acid (PTA). (A) Wild-type (WT) HBsAgS VLPs; (B) N146Q-HBsAgS VLPs; (C) T116N-HBsAgS VLPs; (D) G130N-HBsAgS VLPs.

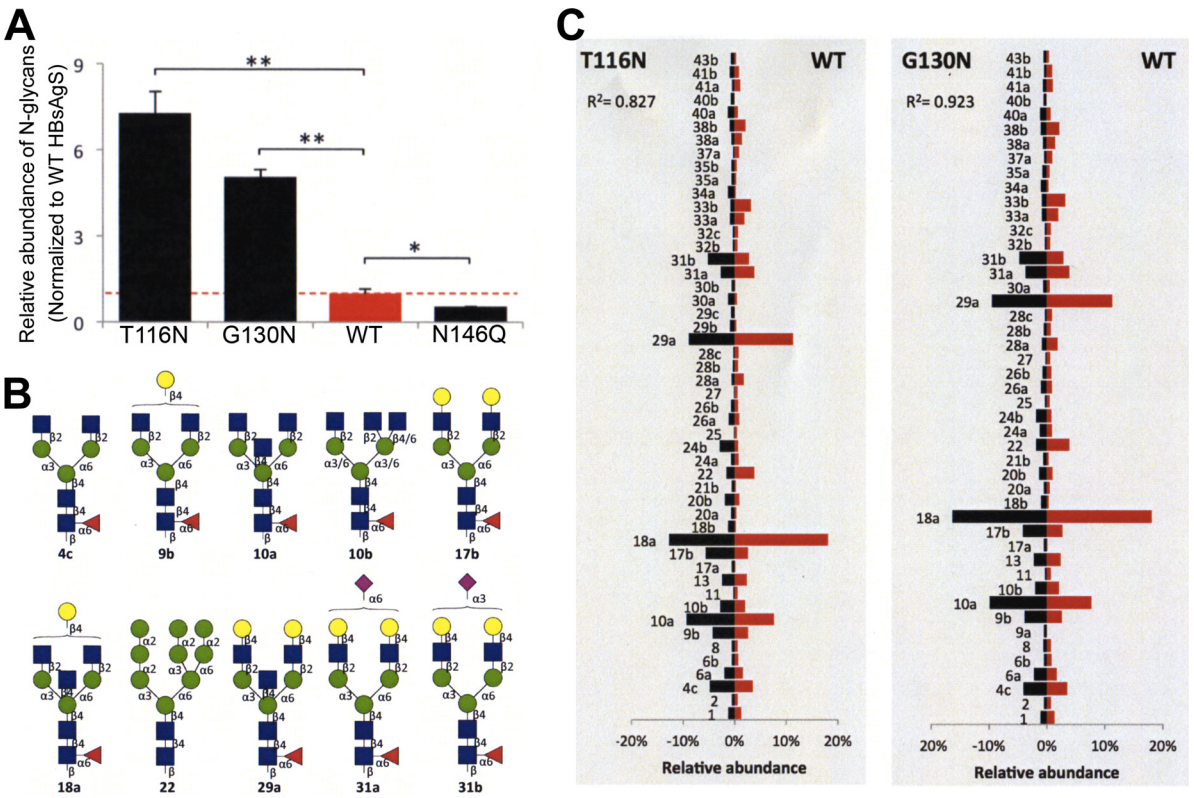

FIG 4 (A) *N*-Glycan abundance of HBsAgS variants as measured by the protein *N*-glycan mass spectrometry (MS) intensity of HBsAgS variants normalized to the wild-type (WT) HBsAgS level (red broken line). (B) Structures of the 10 most abundant glycoforms of HBsAgS. Symbols and nomenclature are according to the Consortium for Functional Glycomics (CFG) convention. Means ± SDs are represented in panels A and C *, $P < 0.05$; **, $P < 0.01$. (C) Relative *N*-glycan structure distribution on WT HBsAgS versus T116N HBsAgS (left) and G130N (right). Only *N*-glycans which were present at more than 0.5% of the total *N*-glycome in at least one of the HBsAgS variants were included in the quantitative distribution (see Table S1 in the supplemental material for all glycan structures). High correlation coefficients (R^2) indicate similar *N*-glycomes. Symbols for the monosaccharides are as follows: for galactose, yellow circles; for mannose, green circles; for *N*-acetylglucosamine, blue squares; for fucose, red triangles; and for *N*-acetylneuraminic acid, purple diamonds. The linkages are indicated.

strates that the variants are predominantly distinguished by a higher *N*-glycan abundance per HBsAgS subunit, and not by different glycan types.

Antigenicity of the differentially glycosylated VLPs. To assess whether the presence of the additional *N*-glycans at amino acid position 116 or 130 influences the binding of anti-HBsAgS antibodies to the VLPs, a collection of 19 monoclonal antibodies directed against HBsAgS was used to monitor antigenic differences of WT and biochemically modified VLPs (Fig. 5). Comparing WT and hyperglycosylayted VLPs, the majority of antibodies directed against loop 1 and loop 2 of the external region, and directed against the N- and C-terminal regions, did not show binding differences indicating that HBsAgS antigenicity has been retained, and substantial shielding of epitopes is avoided. However, three monoclonal antibodies show differences in binding to the modified VLPs, indicating that structural changes and/or restrictions to access the antigenic site have occurred. MAb 5 (loop 1-5) compared to MAb 9 (conform-9) and MAb 11 (loop 2-11) show opposite binding outcomes; MAb 5 (loop 1 epitope) has reduced binding to hypoglycosylated N146Q-ΔHBsAgS VLPs, indicating that the absence of glycan residues in the loop 2 region and/or the amino acid substitution correlates with loss of epitope recognition, possibly due to structural changes compromising antibody binding. In contrast, MAb 9 (conformational epitope) and MAb 11 (loop 2 epitope) bind to hypoglycosylated N146Q-ΔHBsAgS VLPs but showed reduced binding to VLPs with the additional glycans at T116N or G130N, indicating that a higher glycan abundance may compromise access to the antigenic site. Binding of MAb 7 (loop 2-7) is multifaceted and highly sensitive to both hypo- and hyperglycosylation. The absence of the WT N146 residue and the glycans resulted in a loss of binding to the N146Q-ΔHBsAgS VLPs, indicating that glycosylation site 146 and/or the glycans are part of the epitope. But binding is also inhibited in the presence of the WT N146 glycosylation site and an increased glycan abundance due to the presence of the site T116N or G130N, suggesting that the epitope is less accessible on the hyperglycosylated VLPs. The ability of the majority of MAbs to detect hypo- and hyperglycosylated VLPs demonstrates that biochemically modified VLPs have retained HBsAgS-specific antigenicity with exposed B-cell epitopes, a prerequisite for the generation of anti-HBsAgS antibody responses.

Immunogenicity of differentially *N*-glycosylated HBsAgS VLPs. To test whether the presence of additional *N*-glycans influences the immunogenicity of the VLPs, BALB/c mice were immunized with N146Q-ΔHBsAgS, T116N, G130N, and WT VLPs in the absence of an adjuvant. The mice were immunized subcutaneously four times with 2 μg of VLPs in 2-week intervals and then bled each week after each immunization, and after completion of

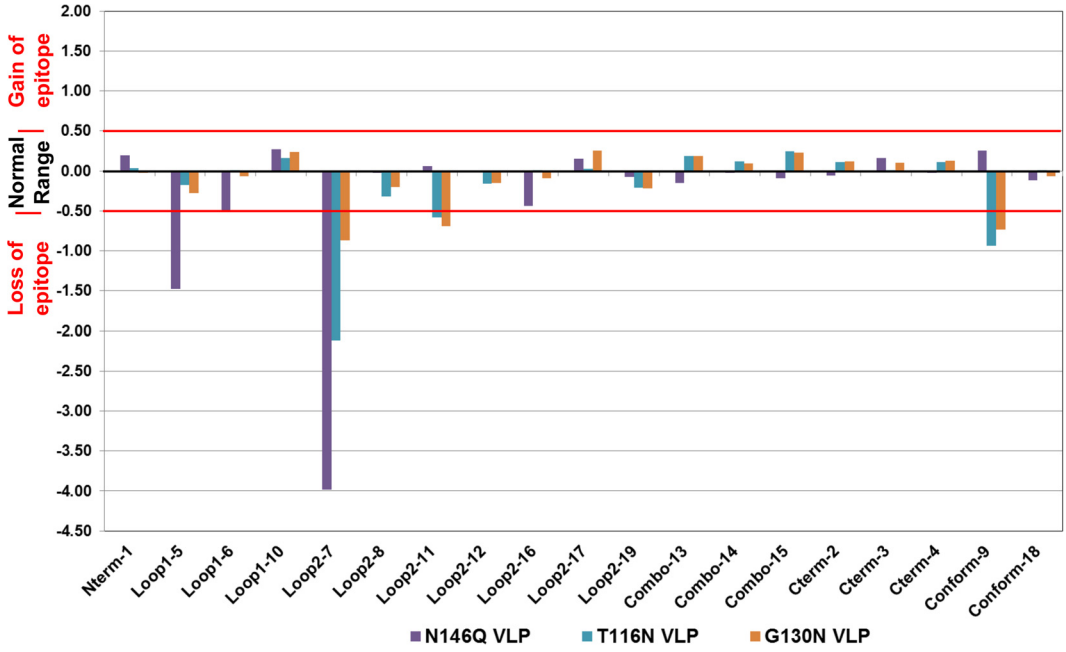

FIG 5 Mapping of the antigenic profile of the HBsAgS VLPs using the Bio-Plex bead-based flow cytometric platform (Bio-Rad, Hercules, CA). The HBsAgS multiplex antibody panel consists of 19 monoclonal antibodies (MAbs) directed against epitopes located between residues 99 and 226 of HBsAgS. The *x* axis defines the HBsAgS region of antibody binding, Nterm, N-terminal region preceding loop 1 domain; loop 1, amino acids 107 to 138; loop 2, amino acids 139 to 149; Combo, semiconformational loop 1/2 epitope; Cterm, C-terminal region amino acids 160 to 226; Conform, conformational epitope. The number after the hyphen stands for the antibody. The *y* axis shows the ratio of antibody binding to wild-type (WT) VLPs versus N146Q VLPs, T116N VLPs, or G130N VLPs. A gain-of-epitope recognition corresponds to positive fold change (>0.5-fold), and loss or reduction of epitope binding corresponds to negative fold changes (>0.5-fold), a range larger or smaller than the variation of epitope recognition of WT VLPs.

the immunization schedule, blood samples were taken weekly until week 13 after the last immunization. The presence of anti-HBsAgS antibodies was detected using an ELISA with yeast-derived VLPs as targets. Using the immunogen T116N VLPs, anti-HBs immune responses were detected in all immunized mice 1 week after the second immunization, with an average anti-HBs titer of 1:900, which is significantly different from the immunization outcomes with WT HBsAgS VLPs ($P < 0.01$) (Fig. 6A). Mice immunized with WT or G130N (hyperglycosylated) HBsAgS VLPs developed anti-HBsAgS antibody titers up to 1:400 or did not show an anti-HBsAgS immune response at an early stage of the immunization schedule (Fig. 6A). Six of eight mice in the test group immunized with G130N VLPs showed anti-HBsAgS antibodies, with an average anti-HBs antibody titer of 1:500. The outcome was not statistically significant compared to the outcomes achieved with the WT and N146Q-ΔHBsAgS VLP immunogens but showed a trend of an earlier antibody response. The outcomes indicate that glycan occupancy of HBsAgS correlates with the immunogenicity. T116N VLPs were able to induce accelerated antibody responses, and G130N VLPs showed a trend toward an enhanced early immune response. The third blood sampling performed 1 week after the third immunization (week 7) showed that anti-HBsAgS-positive mice were detectable in all four test groups, with average antibody titers between 1:1,600 (group immunized with N146Q-ΔHBsAgS VLPs) and 1:3,500 (group immunized with T116N VLPs) (Fig. 6B). High antibody titers persisted, and at 7 weeks after the last immunization (week 14 in the schedule), the group of mice immunized with T116N VLPs had an average anti-HBs titer of 1:9,000, statistically significant compared to the WT group, with an average titer of 1:2,700 (WT VLPs) ($P < 0.01$) (Fig. 6C). The data demonstrate that the T116N VLPs with the highest glycan abundance maintain high antibody titers for a longer period in addition to the induced accelerated anti-HBsAgS antibody response. At 13 weeks after the last immunization (week 20 in the schedule), the final bleed was taken and the average anti-HBsAgS antibody titers were measured; no statistical significance could be determined. The average antibody titers were 1:1,600 (WT VLP), 1:1,700 (N146Q-ΔHBsAgS VLP), 1:2,700 (T116N VLPs), and 1:5,000 (G130N VLPs) (Fig. 6D). Cytotoxic T lymphocyte (CTL) activity was measured at two different time points, 1 and 4 weeks after immunization of BALB/c mice with the different VLP types resulting in CTL responses, which were not significantly different (data not shown), indicating that the cellular immune response against HBsAgS VLPs is possibly dictated by protease sensitivity and antigen processing (34).

The results demonstrate that the presence of additional glycan residues does not efficiently shield HBsAgS-specific B cell epitopes and has the ability to increase the HBsAgS-specific immunogenicity. The ability to generate biochemically modified immunogens with enhanced immunogenicity may allow new avenues for the development of optimized preventive vaccine approaches.

DISCUSSION

In order to enhance or to modulate the immunogenicity of the HBsAgS VLP immunogens, biochemically modified VLPs distinguished by an altered level of protein *N*-glycosylation were generated. The status of *N*-glycosylation can influence the interaction of

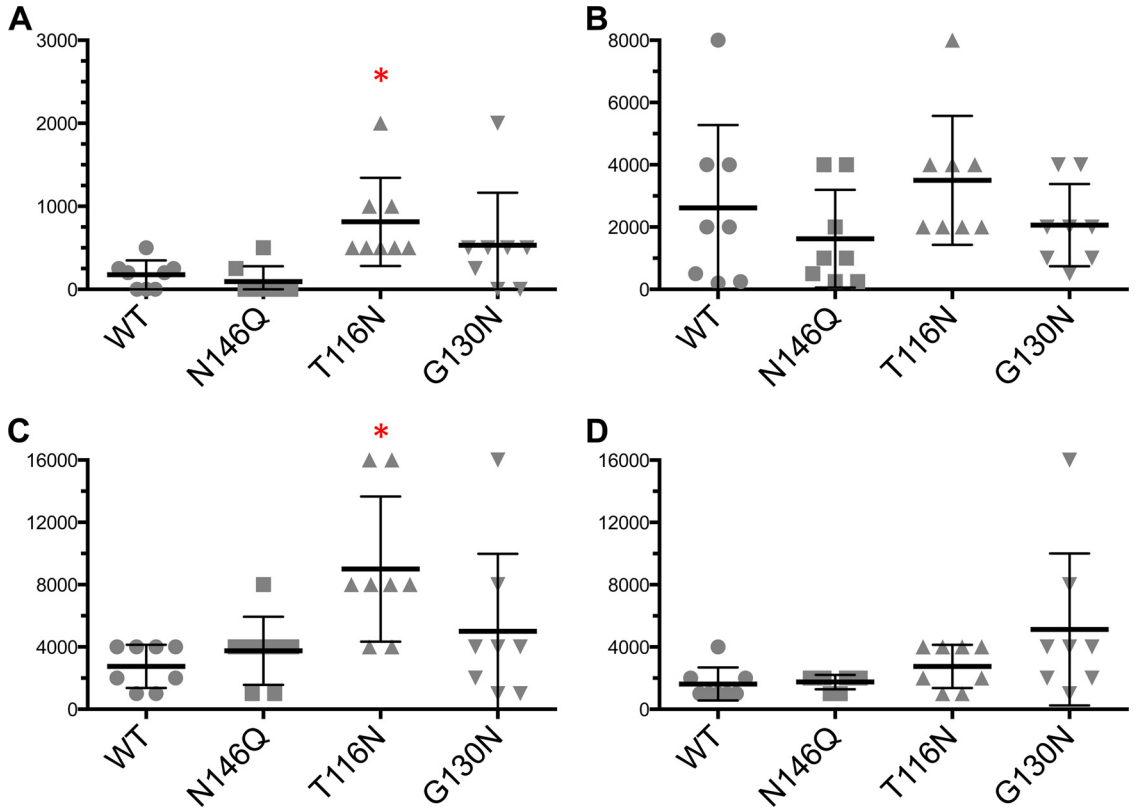

FIG 6 Groups of eight BALB/c mice were immunized with 2 μg of VLPs in weeks 1, 3, 5, and 7 in the absence of adjuvant. Serum samples were taken in week 4 (A), week 6 (B), and week 14 (C) and at the last bleed in week 20 (D). HBsAgS-specific antibody responses were measured by an enzyme-linked immunosorbent assay (ELISA) against yeast-derived HBsAg VLPs (serotype ayw). Endpoint titer was determined to be the highest serum dilution that gave an optical density OD value of at least two times above background. Standard deviations were calculated and are indicated as error bars. The red asterisk indicates that the difference between the T116N VLPs and WT VLPs is statistically significant ($P < 0.01$).

the immunogen with antigen-presenting cells (36–38). It is recognized that *N*-glycans are relatively large molecular entities, which decorate higher protein structures and may therefore contribute to particle uptake and processing by antigen-presenting cells. Recognition of glycans expressed on pathogens by host lectins is dictated by the nature, spatial presentation, and abundance of the glycans. The polyvalent display of glycan epitopes on pathogens seems to facilitate lectin binding (43). The ability of the lectin actinohivin to recruit three high-mannose-type glycans, which are present at high density on the human immunodeficiency virus type 1 (HIV-1) envelope protein gp120, seems to be essential for an efficient blocking of HIV-1 infection of target cells (63). An enhanced uptake of hyperglycosylated VLPs derived from the rabbit hemorrhagic disease virus (RHDV) by antigen-presenting cells strongly indicates that the interaction between an antigen and immune cells can be modified depending on the glycosylation status of the antigen (38). Utilizing glycans and targeting lectin receptors to promote antigen uptake and presentation is a promising path to enhance subsequent antigen-specific immune responses (40, 46, 64).

To modify the immunogenicity of the HBsAgS VLPs, we successfully generated hyperglycosylated VLPs. The introduction of new *N*-glycosylation sites by replacing the amino acid residues threonine at position 116 or glycine at position 130 with asparagine residues reconstituted the consensus sequence Asn-X-Ser/Thr. Both sites are exposed within the external and antigenic HBsAgS loop region and should be accessible by the oligosaccharyl transferase (OST) for the first initiating step of *N*-glycosylation in the ER. The location of an additional site of glycosylation at position 116 or 130 increased the *N*-glycan occupancy on the HBsAgS VLPs, with the T116N site being more efficiently glycosylated than the G130N site. This is consistent with the finding by Julithe et al. (31) that the *N*-glycosylation site closer to the N terminus is more efficiently glycosylated than sites closer to the C-terminal end.

Despite differences regarding the glycosylation efficiency between amino acids 116 and 130 and the WT (N146), LC-MS/MS analysis showed that the nature of the *N*-glycans at these sites is generally similar when assessed by *N*-glycome profiling, and predominately of a complex type, abundantly showing immune-important determinants, including the previously unreported dominance of bisecting GlcNAc residues and core fucosylation (Fig. 4). However, detailed glycopeptide site-specific analysis of HBsAgS may still reveal significant site-specific variations in the structure of the glycans (core fucosylation, Lewis-type fucosylation, sialylation, and bisecting GlcNAc) between WT and the glycosylation variants of HBsAgS, aspects we are pursuing using a recently developed approach (65). The N146Q-ΔHBsAgS VLPs contained trace levels of oligomannose possibly attached to the N-terminal NH_2-1-MENIT-5 sequence. The N3 position is not efficiently recognized in HBsAgS VLPs, possibly due to the proximity of a transmembrane region and lipids, which may interfere with the pro-

cessing and maturation steps to generate complex glycans (66, 67). To assess whether the biochemically modified VLPs have retained HBsAgS-specific antigenicity, a panel of 19 anti-HBsAgS-specific MAbs were used and tested for their ability to bind to the modified VLPs versus WT VLPs. The outcome demonstrated that HBsAgS-specific antigenicity has been retained: 15 out of 19 anti-HBsAgS antibodies recognize the hyperglycosylated VLPs regardless of the presence of the additional glycosylation sites at position 116 or 130. Loss of epitope recognition by the MAbs 7, 9, and 11 is most likely due to the restricted access to the antigenic site on the hyperglycosylated T116N- and G130N-HBsAgS VLPs. The loss of binding of the loop 2-specific MAbs 7 and 11 to T116N-HBsAgS VLPs that contain additional glycans in the loop 1 region indicates that reduced or occluded epitope access most likely prevents recognition of the VLPs. MAb 7 seems to recognize its epitope in a highly glycosylation-sensitive manner, with epitope recognition or access reduced in the context of both hypo- and hyperglycosylated VLPs, with loss of epitopes by N146Q-ΔHBsAgS and also for the WT N146 site in the presence of additional glycan residues at either position 116 or 130. The immunization studies are consistent with the antigenicity studies; both T116N- and G130N-HBsAgS VLPs induce anti-HBsAgS-specific immune responses, highlighting the accessibility of the B cell epitopes in the context of hyperglycosylated VLPs. Mice immunized with the T116N VLPs induce earlier immune responses, which is statistically significant, followed by the G130N VLPs, which show a trend of an earlier response than for WT and nonglycosylated VLPs. The induction of an earlier and longer-lasting anti-HBsAgS antibody response correlates with the increased glycan abundance of the HBsAgS VLPs. Because of the presence of the same glycan types on the WT, T116N, and G130N VLPs, we do not expect that the hyperglycosylated VLPs interact with different sets of antigen-presenting cells by engaging different lectin receptors but follow the uptake pathway of the WT VLPs. The hyperglycosylated VLPs are possibly more efficiently taken up by antigen-presenting cells to allow an earlier and longer-lasting B cell immune response.

To investigate HBV immune escape, Yu et al. (68) analyzed a cohort of chronically infected patients with coexisting HBsAgS protein and anti-HBs antibodies, and they demonstrated the presence of HBV mutants encoding HBsAgS with additional glycosylation sites. An increased frequency of new *N*-glycosylation sites within the external hydrophilic loop region, predominately at the positions 129 and 131, reduced antigenicity and possibly facilitated viral escape. Our assay system demonstrated that binding of three antibodies (7, 9, and 11) out of 19 to hyperglycosylated VLPs is reduced, possibly indicating that the quality of the B cell immune response during a natural infection may allow escape. The presence of anti-HBsAgS antibodies not able to engage hyperglycosylated particles during an ongoing infection may thus facilitate the escape of mutant viruses with additional glycosylation sites. A broad B cell immune response generating antibodies able to engage hyperglycosylated VLPs may reduce the risk of escape of HBV mutants with higher glycan density.

The importance of glycosylation for the improvement of recombinant biopharmaceuticals and immunogenic properties has been recognized (69). To develop further superior vaccination approaches, investigating synergistic effects of biochemically modified immunogens and adjuvants acceptable for usage in humans possibly represents an avenue for the generation of optimized vaccines and delivery platforms.

ACKNOWLEDGMENTS

H.J.N. was supported by a grant awarded by the Australian Centre for HIV and Viral Hepatitis Research (ACH^2). M.T.-A. was supported by the Early Career Development Program, Cancer Institute, NSW, Australia. N.H.P. acknowledges the support of ARC Discovery Grant DP110104958.

REFERENCES

1. **Buonaguro L, Tagliamonte M, Tornesello ML, Buonaguro FM.** 2011. Developments in virus-like particle-based vaccines for infectious diseases and cancer. Expert Rev Vaccines **10:**1569–1583. http://dx.doi.org/10.1586/erv.11.135.
2. **Jennings GT, Bachmann MF.** 2009. Immunodrugs: therapeutic VLP-based vaccines for chronic diseases. Annu Rev Pharmacol Toxicol **49:**303–326. http://dx.doi.org/10.1146/annurev-pharmtox-061008-103129.
3. **Pushko P, Pumpens P, Grens E.** 2013. Development of virus-like particle technology from small highly symmetric to large complex virus-like particle structures. Intervirology **56:**141–165. http://dx.doi.org/10.1159/000346773.
4. **Jilg W, Schmidt M, Zoulek G, Lorbeer B, Wilske B, Deinhardt F.** 1984. Clinical evaluations of a recombinant HBV vaccine. Lancet **ii:**1174–1175.
5. **Zuckerman JN.** 2006. Protective efficacy, immunotherapeutic potential, and safety of hepatitis B vaccines. J Med Virol **78:**169–177. http://dx.doi.org/10.1002/jmv.20524.
6. **Busch K, Thimme R.** 2015. Natural history of chronic hepatitis B virus infection. Med Microbiol Immunol **204:**5–10. http://dx.doi.org/10.1007/s00430-014-0369-7.
7. **World Health Organization.** 2013. Hepatitis B. Fact sheet no. 204, updated July 2013. World Health Organization, Geneva, Switzerland.
8. **Akbar SMF, Furukawa S, Horiike N, Abe M, Hiasa Y, Onji M.** 2011. Safety and immunogenicity of hepatitis B surface antigen pulsed dendritic cells in patients with chronic hepatitis B. J Viral Hepat **18:**408–414.
9. **Bertoletti A, Gehring AJ.** 2013. Immune therapeutic strategies in chronic hepatitis B virus infection: virus or inflammation control? PLoS Pathog **9:**e1003784. http://dx.doi.org/10.1371/journal.ppat.1003784.
10. **Moffat JM, Cheong W-S, Villadangos JA, Mintern JD, Netter HJ.** 2013. Hepatitis B virus-like particles access major histocompatibility class I and II antigen presentation pathways in primary dendritic cells. Vaccine **31:**2310–2316. http://dx.doi.org/10.1016/j.vaccine.2013.02.042.
11. **Beaumont E, Patient R, Hourioux C, Dimier-Poisson I, Roingeard P.** 2013. Chimeric hepatitis B virus/hepatitis C virus envelope proteins elicit broadly neutralizing antibodies and constitute a potential bivalent prophylactic vaccine. Hepatology **57:**1303–1313. http://dx.doi.org/10.1002/hep.26132.
12. **Cheong W-S, Reiseger J, Turner SJ, Boyd R, Netter HJ.** 2009. Chimeric virus-like particles for the delivery of an inserted conserved influenza A-specific CTL epitope. Antiviral Res **81:**113–122. http://dx.doi.org/10.1016/j.antiviral.2008.10.003.
13. **Cheong W-S, Drummer HE, Netter HJ.** 2009. Delivery of a foreign epitope by sharing amino acid residues with the carrier matrix. J Virol Methods **158:**35–40. http://dx.doi.org/10.1016/j.jviromet.2009.01.015.
14. **Delpeyroux F, Chenciner N, Lim A, Malpiece Y, Blondel B, Crainic R, van der Werf S, Streeck RE.** 1986. A poliovirus neutralization epitope expressed on hybrid hepatitis B surface antigen particles. Science **233:**472–475. http://dx.doi.org/10.1126/science.2425433.
15. **Michel M, Lone Y-C, Centlivre M, Roux P, Wain-Hobson S, Sala M.** 2007. Optimisation of secretion of recombinant HBsAg virus-like particles: impact on the development of HIV-1/HBV bivalent vaccines. Vaccine **25:**1901–1911. http://dx.doi.org/10.1016/j.vaccine.2006.08.014.
16. **Netter HJ, Macnaughton TB, Woo W-P, Tindle R, Gowans EJ.** 2001. Antigenicity and immunogenicity of novel chimeric hepatitis B surface antigen particles with exposed hepatitis C virus epitopes. J Virol **75:**2130–2141. http://dx.doi.org/10.1128/JVI.75.5.2130-2141.2001.
17. **Phogat S, Svehla K, Tang M, Spadaccini A, Muller J, Mascola J, Berkower I, Wyatt R.** 2008. Analysis of the human immunodeficiency virus type 1 gp41 membrane proximal external region arrayed on hepatitis B surface antigen particles. Virology **373:**72–84. http://dx.doi.org/10.1016/j.virol.2007.11.005.
18. **Vietheer PTK, Boo I, Drummer HE, Netter HJ.** 2007. Immunisations with chimeric hepatitis B VLPs to induce potential anti-hepatitis C virus neutralising antibodies. Antivir Ther **12:**477–487.
19. **Regules JA, Cummings JF, Ockenhouse CF.** 2011. The RTS,S vaccine candidate for malaria. Expert Rev Vaccines **10:**589–599. http://dx.doi.org/10.1586/erv.11.57.

20. **RTS,S Clinical Trials Partnership.** 2014. Efficacy and safety of the RTS,S/AS01 malaria vaccine during 18 months after vaccination: a phase 3 randomized, controlled trial in children and young infants at 11 African sites. PLoS Med **11:**e1001685. http://dx.doi.org/10.1371/journal.pmed.1001685.
21. **Stirk HJ, Thornton JM, Howard CR.** 1992. A topological model for hepatitis B surface antigen. Intervirology **33:**148–158.
22. **Carman WF, Owsianka A, Wallace LA, Dow BC, Mutimer DJ.** 1999. Antigenic characterisation of pre- and post-liver transplant hepatitis B surface antigen sequences from patients treated with hepatitis B immune globulin. J Hepatol **31:**195–201. http://dx.doi.org/10.1016/S0168-8278(99)80213-X.
23. **Weinberger KM, Bauer T, Böhm S, Jilg W.** 2000. High genetic variability of the group-specific *a*-determinant of hepatitis B virus surface antigen (HBsAg) and the corresponding fragment of the viral polymerase in chronic virus carriers lacking detectable HBsAg in serum. J Gen Virol **81:**1165–1174. http://dx.doi.org/10.1099/0022-1317-81-5-1165.
24. **Greiner VJ, Egelé C, Oncul S, Ronzon F, Manin C, Klymchenko A, Mély Y.** 2010. Characterization of the lipid and protein organization in HBsAg viral particles by steady-state and time-resolved fluorescence spectroscopy. Biochimie **92:**994–1002. http://dx.doi.org/10.1016/j.biochi.2010.04.014.
25. **Mangold CM, Unckell F, Werr M, Streeck RE.** 1997. Analysis of intermolecular disulfide bonds and free sulfhydryl groups in hepatitis B surface antigen particles. Arch Virol **142:**2257–2267. http://dx.doi.org/10.1007/s007050050240.
26. **Wunderlich G, Bruss V.** 1996. Characterization of early hepatitis B virus surface protein oligomers. Arch Virol **141:**1191–1205. http://dx.doi.org/10.1007/BF01718824.
27. **Mehta A, Lu X, Block TM, Blumberg BS, Dwek RA.** 1997. Hepatitis B virus (HBV) envelope glycoproteins vary drastically in their sensitivity to glycan processing: evidence that alteration of a single N-linked glycosylation site can regulate HBV secretion. Proc Natl Acad Sci U S A **94:**1822–1827. http://dx.doi.org/10.1073/pnas.94.5.1822.
28. **Gillece-Castro BL, Fisher SJ, Tarentino AL, Peterson DL, Burlingame AL.** 1987. Structure and the oligosaccharide portion of human hepatitis B surface antigen. Arch Biochem Biophy **256:**194–201. http://dx.doi.org/10.1016/0003-9861(87)90437-1.
29. **Hanaoka K, Takasaki S, Kobata A, Miyamoto H, Nakamura T, Mayumi M.** 1986. Structure of asparagine-linked sugar chains in the major polypeptide of hepatitis B surface antigen. J Biochem **99:**1273–1276.
30. **Ito K, Qin Y, Guarnieri M, Garcia T, Kwei K, Mizokami M, Zhang J, Li J, Wands JR, Tong S.** 2010. Impairment of hepatitis B virus virion secretion by single-amino-acid substitutions in the small envelope protein and rescue by a novel glycosylation site. J Virol **84:**12850–12861. http://dx.doi.org/10.1128/JVI.01499-10.
31. **Julithe R, Abou-Jaoudé G, Sureau C.** 2014. Modification of the hepatitis B virus envelope protein glycosylation pattern interferes with secretion of viral particles, infectivity, and susceptibility to neutralizing antibodies. J Virol **88:**9049–9059. http://dx.doi.org/10.1128/JVI.01161-14.
32. **Lu X, Mehta A, Dwek R, Butters T, Block T.** 1995. Evidence that N-linked glycosylation is necessary for hepatitis B virus secretion. Virology **213:**660–665. http://dx.doi.org/10.1006/viro.1995.0038.
33. **Patzer EJ, Nakamura GR, Yaffe A.** 1984. Intracellular transport and secretion of hepatitis B surface antigen in mammalian cells. J Virol **51:**346–353.
34. **Cheong W-S, Hyakumura M, Yuen L, Warner N, Locarnini S, Netter HJ.** 2012. Modulation of the immunogenicity of virus-like particles composed of mutant hepatitis B virus envelope subunits. Antiviral Res **93:**209–218. http://dx.doi.org/10.1016/j.antiviral.2011.11.011.
35. **Li P, Haque MA, Blum JS.** 2002. Role of disulfide bonds in regulating antigen processing and epitope selection. J Immunol **169:**2444–2450. http://dx.doi.org/10.4049/jimmunol.169.5.2444.
36. **Mirano-Bascos D, Steede K, Robinson JE, Landry SJ.** 2010. Influence of disulfide-stabilized structure on the specificity of helper T-cell and antibody responses to HIV envelope glycoprotein gp120. J Virol **84:**3303–3311. http://dx.doi.org/10.1128/JVI.02242-09.
37. **Prato S, Fleming J, Schmidt CW, Corradin G, Lopez JA.** 2006. Cross-presentation of a human malaria CTL epitope is conformation dependent. Mol Immunol **43:**2031–2036. http://dx.doi.org/10.1016/j.molimm.2005.12.014.
38. **Al-Barwani F, Young SL, Baird MA, Larsen DS, Ward VK.** 2014. Mannosylation of virus-like particles enhances internalization by antigen presenting cells. PLoS One **9:**e104523. http://dx.doi.org/10.1371/journal.pone.0104523.
39. **Freire T, Zhang X, Dériaud E, Ganneau C, Vichier-Guerre S, Azria E, Launay O, Lo-Man R, Bay S, Leclerc C.** 2010. Glycosidic Tn-based vaccines targeting dermal dendritic cells favor germinal center B-cell development and potent antibody response in the absence of adjuvant. Blood **116:**3526–3536. http://dx.doi.org/10.1182/blood-2010-04-279133.
40. **Sheng KC, Kalkanidis M, Pouniotis DS, Esparon S, Tang CK, Apostolopoulos V, Pietersz GA.** 2008. Delivery of antigen using a novel mannosylated dendrimer potentiates immunogenicity in vitro and in vivo. Eur J Immunol **38:**424–436. http://dx.doi.org/10.1002/eji.200737578.
41. **Doe B, Steimer KS, Walker CM.** 1994. Induction of HIV-1 envelope (gp120)-specific cytotoxic T lymphocyte responses in mice by recombinant CHO cell-derived gp120 is enhanced by enzymatic removal of N-linked glycans. Eur J Immunol **24:**2369–2376. http://dx.doi.org/10.1002/eji.1830241017.
42. **Vigerust DJ, Shepherd VL.** 2007. Virus glycosylation: role in virulence and immune interactions. Trends Microbiol **15:**211–218. http://dx.doi.org/10.1016/j.tim.2007.03.003.
43. **Dam TK, Brewer CF.** 2010. Lectins as pattern recognition molecules: the effects of epitope density in innate immunity. Glycobiology **20:**270–279. http://dx.doi.org/10.1093/glycob/cwp186.
44. **Wolfert MA, Boons G-J.** 2013. Adaptive immune activation: glycosylation does matter. Nat Chem Biol **9:**776–784. http://dx.doi.org/10.1038/nchembio.1403.
45. **Gazi U, Martinez-Pomares L.** 2009. Influence of the mannose receptor in host immune responses. Immunobiology **214:**554–561. http://dx.doi.org/10.1016/j.imbio.2008.11.004.
46. **Hamdy S, Haddadi A, Shayeganpour A, Samuel J, Lavasanifar A.** 2011. Activation of antigen-specific T cell-responses by mannan-decorated PLGA nanoparticles. Pharm Res **28:**2288–2301. http://dx.doi.org/10.1007/s11095-011-0459-9.
47. **Yao W, Peng Y, Du M, Luo J, Zong L.** 2013. Preventative vaccine-loaded mannosylated chitosan nanoparticles intended for nasal mucosal delivery enhance immune responses and potent tumor immunity. Mol Pharm **10:**2904–2914. http://dx.doi.org/10.1021/mp4000053.
48. **Mishra H, Mishra D, Mishra PK, Nahar M, Dubey V, Jain NK.** 2010. Evaluation of solid lipid nanoparticles as carriers for delivery of hepatitis B surface antigen for vaccination using subcutaneous route. J Pharm Pharm Sci **13:**495–509.
49. **Lim LY, Yuen L, Hammond R, Angus PW, Thompson AJ, Patterson S, Leary T, Yin P, Thomas H, Locarnini S, Walsh R.** 2014. Mapping the HBsAg immune phenotype to predict HBsAg loss or decline in chronic hepatitis B in patients receiving nucleot(s)ide analogue therapy, abstr 1623. Hepatology **60**(Suppl 1)**:**980A.
50. **Jolivet-Reynaud C, Lésenéchal M, O'Donnell B, Becquart L, Foussadier A, Forge F, Battail-Poirot N, Lacaux X, Carman W, Jolivet M.** 2001. Localization of hepatitis B surface antigen epitopes present on variants and specifically recognised by anti-hepatitis B surface antigen monoclonal antibodies. J Med Virol **65:**241–249. http://dx.doi.org/10.1002/jmv.2026.
51. **Paulij WP, de Wit PL, Sünnen CM, van Roosmalen MH, Petersen-van Ettekoven A, Cooreman MP, Heijtink RA.** 1999. Localization of a unique hepatitis B virus epitope sheds new light on the structure of hepatitis B virus surface antigen. J Gen Virol **80:**2121–2126. http://dx.doi.org/10.1099/0022-1317-80-8-2121.
52. **Eren R, Lubin I, Terkieltaub D, Ben-Moshe O, Zauberman A, Uhlmann R, Tzahor T, Moss S, Ilan E, Shouval D, Galun E, Daudi N, Marcus H, Reisner Y, Dagan S.** 1998. Human monoclonal antibodies specific to hepatitis B virus generated in a human/mouse radiation chimera: the Trimera system. Immunology **93:**154–161.
53. **Waters JA, Brown SE, Steward MW, Howard CR, Thomas HC.** 1991. Analysis of the antigenic epitopes of hepatitis B surface antigen involved in the induction of a protective antibody response. Virus Res **22:**1–12.
54. **Chen Y-CJ, Delbrook K, Dealwis C, Mimms L, Mushahwar IK, Mandecki W.** 1996. Discontinous epitopes of hepatitis B surface antigen derived from a filamentous phage peptide library. Proc Natl Acad Sci U S A **93:**1997–2001. http://dx.doi.org/10.1073/pnas.93.5.1997.
55. **Jensen PH, Karlsson NG, Kolarich D, Packer NH.** 2012. Structural analysis of N- and O-glycans released from glycoproteins. Nat Protoc **7:**1299–1310. http://dx.doi.org/10.1038/nprot.2012.063.
56. **Sethi MK, Thaysen-Andersen M, Smith JT, Baker MS, Packer NH, Hancock WS, Fanayan S.** 2014. Comparative N-glycan profiling of colorectal cancer cell lines reveals unique bisecting GlcNAc and α-2,3-linked

sialic acid determinants are associated with membrane proteins of the more metastatic/aggressive cell lines. J Proteome Res **13:**277–288. http://dx.doi.org/10.1021/pr400861m.

57. **Venkatakrishnan V, Thaysen-Andersen M, Chen SC, Nevalainen H, Packer NH.** 2015. Cystic fibrosis and bacterial colonization define the sputum N-glycosylation phenotype. Glycobiology **25:**88–100. http://dx.doi.org/10.1093/glycob/cwu092.
58. **Moh ES, Thaysen-Andersen M, Packer NH.** 2015. Relative versus absolute quantitation in disease glycomics. Proteomics Clin Appl http://dx.doi.org/10.1002/prca.201400184.
59. **Leymarie N, Griffin PJ, Jonscher K, Kolarich D, Orlando R, McComb M, Zaia J, Aguilan J, Alley WR, Altmann F, Ball LE, Basumallick L, Bazemore-Walker CR, Behnken H, Blank MA, Brown KJ, Bunz SC, Cairo CW, Cipollo JF, Daneshfar R, Desaire H, Drake RR, Go EP, Goldman R, Gruber C, Halim A, Hathout Y, Hensbergen PJ, Horn DM, Hurum D, Jabs W, Larson G, Ly M, Mann BF, Marx K, Mechref Y, Meyer B, Möginger U, Neusüß C, Nilsson J, Novotny MV, Nyalwidhe JO, Packer NH, Pompach P, Reiz B, Resemann A, Rohrer JS, Ruthenbeck A, Sanda M, Schulz JM, Schweiger-Hufnagel U, Sihlbom C, Song E, Staples GO, Suckau D, Tang H, Thaysen-Andersen M, Viner RI, An Y, Valmu L, Wada Y, Watson M, Windwarder M, Whittal R, Wuhrer M, Zhu Y, Zou C.** 2013. Interlaboratory study on differential analysis of protein glycosylation by mass spectrometry: the ABRF glycoprotein research multi-institutional study 2012. Mol Cell Proteomics **12:**2935–2951. http://dx.doi.org/10.1074/mcp.M113.030643.
60. **Dubois MF, Pourcel C, Rousset S, Chany C, Tiollais P.** 1980. Excretion of hepatitis B surface antigen particles from mouse cells transformed with cloned viral DNA. Proc Natl Acad Sci U S A **77:**4549–4553. http://dx.doi.org/10.1073/pnas.77.8.4549.
61. **Moriarty AM, Hoyer BH, Shih JW, Gerin JL, Hamer DH.** 1981. Expression of the hepatitis B virus surface antigen gene in cell culture using a simian virus 40 vector. Proc Natl Acad Sci U S A **78:**2606–2610. http://dx.doi.org/10.1073/pnas.78.4.2606.
62. **Yuen LK, Ayres A, Littlejohn M, Colledge D, Edgely A, Maskill WJ, Locarnini SA, Bartholomeusz A.** 2007. SeqHepB: a sequence analysis program and relational database system for chronic hepatitis B. Antiviral Res **75:**64–74.
63. **Tanaka H, Chiba H, Inokoshi J, Kuno A, Sugai T, Takahashi A, Ito Y, Tsunoda M, Suzuki K, Takenaka A, Sekiguchi T, Umeyama H, Hirabayashi J, Omura S.** 2009. Mechanism by which the lectin actinohivin blocks HIV infection of target cells. Proc Natl Acad Sci U S A **106:**15633–15638. http://dx.doi.org/10.1073/pnas.0907572106.
64. **Denda-Nagai K, Aida S, Saba K, Suzuki K, Moriyama S, Oo-Puthinan S, Tsuiji M, Morikawa A, Kumamoto Y, Sugiura D, Kudo A, Akimoto Y, Kawakami H, Bovin NV, Irimura T.** 2010. Distribution and function of macrophage galactose-type C-type lectin 2 (MGL2/CD301b): efficient uptake and presentation of glycosylated antigens by dendritic cells. J Biol Chem **285:**19193–19204. http://dx.doi.org/10.1074/jbc.M110.113613.
65. **Thaysen-Andersen M, Packer NH.** 2014. Advances in LC-MS/MS-based glycoproteomics: getting closer to system-wide site-specific mapping of the N- and O-glycoproteome. Biochim Biophys Acta **1844:**1437–1452. http://dx.doi.org/10.1016/j.bbapap.2014.05.002.
66. **Lee LY, Lin C-H, Fanayan S, Packer NH, Thaysen-Andersen M.** 2014. Differential site accessibility mechanistically explains subcellular-specific N-glycosylation determinants. Front Immunol **5:**404.
67. **Thaysen-Andersen M, Packer NH.** 2012. Site-specific glycoproteomics confirms that protein structure dictates formation of N-glycan type, core fucosylation and branching. Glycobiology **22:**1440–1452. http://dx.doi.org/10.1093/glycob/cws110.
68. **Yu D-M, Li X-H, Mom V, Lu Z-H, Liao X-W, Han Y, Pichoud C, Gong Q-M, Zhang D-H, Zhang Y, Deny P, Zoulim F, Zhang X-X.** 2014. N-glycosylation mutations within hepatitis B virus surface major hydrophilic region contribute mostly to immune escape. J Hepatol **60:**515–522. http://dx.doi.org/10.1016/j.jhep.2013.11.004.
69. **Butler M, Spearman M.** 2014. The choice of mammalian cell host and possibilities for glycosylation engineering. Curr Opin Biotechnol **30:**107–112. http://dx.doi.org/10.1016/j.copbio.2014.06.010.